Optica Applicata, Vol. XXXIV, No. 4, 2004

Polarization mode dispersion in birefringent microstructured fibers

TOMASZ R. WOLIŃSKI[1], PIOTR LESIAK[1], KATARZYNA SZANIAWSKA[1],
ANDRZEJ W. DOMAŃSKI[1], JAN WÓJCIK[2]

[1]Faculty of Physics, Warsaw University of Technology, ul. Koszykowa 75, 00-662 Warszawa, Poland;
e-mail: wolinski@if.pw.edu.pl

[2]Faculty of Chemistry, Maria Curie-Sklodowska University (UMCS),
pl. Marii Curie-Skłodowskiej 2, 20-031 Lublin, Poland

The possibility of compensation of polarization mode dispersion (PMD) by using highly birefringent (HB) fibers was proposed a few years ago. In this paper, we present our results of measurement of PMD value in a new type of birefringent microstructred fibers: photonic crystal fibers (PCF). Their low temperature sensitivity and simultaneously high longitudinal strain sensitivity make them possible to be used as PMD compensation components.

Keywords: polarization mode dispersion, birefringent fibers, microstructured fibers.

1. Introduction

Since the early 1990s the interest in the polarization mode dispersion (PMD) has been continuously growing. The main reason is that PMD broadens the pulse of light in the fiber line as a result of residual linear birefringence that is present in a telecommunication fiber. This phenomenon limits the development of a high-speed telecommunication system [1].

Polarization mode dispersion compensators may either limit average value of differential group delay (DGD) or may dynamically limit the actual value of DGD in a telecom line. The most promising setup uses the highly birefringent (HB) fibers as compensation components [2].

Internal linear birefringence could be introduced into a fiber during its manufacturing process. Generally, “classical” HB fibers are characterized either by elliptical cores [3] or by stressed regions near their cores (bow-tie, Panda, side-hole) [4]. In microstructured photonic crystal fibers, birefringence is achieved by breaking the distribution of refractive indices in orthogonal direction of the fiber cross-section.

Different cross-section patterns of HB PCFs have been reported so far [5], [6] and dependence of the modal birefringence on the holes size has been observed [7].

In this work, we present our latest results on PMD measurements in different types of microstructured birefringent fibers. The measurements included two types of highly birefringent photonic crystal fibers in comparison with the *Fibercore* bow-tie fiber. These results are of potential application in perspective construction of an all-fiber PMD compensator.

2. Theoretical background

PMD in a single mode fiber (SMF) has a statistical character [1] and changes as a square root of the fiber length. In an HB fiber there is no mode coupling and in consequence PMD is equal to DGD.

The phase difference in the HB fiber is described by the following formula:

$$\Delta\delta = L(\Delta\beta) = Lk\Delta n_{\mathrm{eff}} \tag{1}$$

where: δ – the phase difference, L – the fiber length, $\Delta\beta$ – the difference between orthogonal propagation constants, k – the wavelength number, and Δn_{eff} – the difference between refractive indices of the orthogonal modes.

Highly birefringent fibers are generally used in fiber optic sensors [8]. For any external perturbation X, the phase difference between both orthogonal polarization components of the HB fiber changes according to:

$$\frac{\partial(\Delta\delta)}{\partial X} = \frac{2\pi}{\lambda}\left(\Delta n_{\mathrm{eff}}\frac{\partial L}{\partial X} + L\,\frac{\partial(\Delta n_{\mathrm{eff}})}{\partial X}\right), \qquad X = T, p, \varepsilon, \ldots \tag{2}$$

where T, p, ε denote temperature, pressure, and longitudinal strain, respectively.

For the longitudinal strain ε changes in birefringence are described by the following formula [8]:

$$\Delta\beta(\varepsilon) = \Delta\beta_0 + \mathrm{sgn}\left\{\frac{\mathrm{d}(\Delta\beta)}{\mathrm{d}\varepsilon}\right\}\varepsilon\,\frac{2\pi}{T_\varepsilon L_i} \tag{3}$$

where: T_ε – an experimentally measurable parameter corresponding to the amount of strain required to induce a 2π phase shift of the polarized light observed at the output, and L_i – the length of the fiber under longitudinal strain. Polarization mode dispersion, usually expressed by differential group delay over the length of the fiber, $\Delta\tau/L$ and modal birefringence $\Delta\beta$ are the most important parameters characterizing birefringent fibers. Both parameters are interrelated according to the formula:

$$\frac{\Delta\tau}{L} = \frac{\mathrm{d}(\Delta\beta)}{\mathrm{d}\omega} = \frac{1}{c}\left(\Delta n_{\mathrm{eff}} + \omega\frac{\mathrm{d}(\Delta n_{\mathrm{eff}})}{\mathrm{d}\omega}\right) \tag{4}$$

where $\Delta\tau/L$ is usually expressed in units of picoseconds per kilometer of fiber length, Δn_{eff} is the differential effective index of refraction for the slow and fast polarization modes, and $\omega = 2\pi c/\lambda$ is the angular frequency of light.

This explains that PMD depends on the phase birefringence as well as on the chromatic dispersion.

3. Microstructured highly birefringent fibers

In our research, we used two different types of highly birefringent photonic crystal fibers presented in Fig. 1. in comparison with the *Fibercore* HB bow-tie fiber (Fig. 1**a**). One of the HB photonics crystal fibers, manufactured in the Optical Fiber Technology Laboratory at the University of Maria Curie-Sklodowska (UMCS), Lublin, Poland (Fig. 1**b**), with air-holes of 0.8 μm in diameter was characterized by the core located

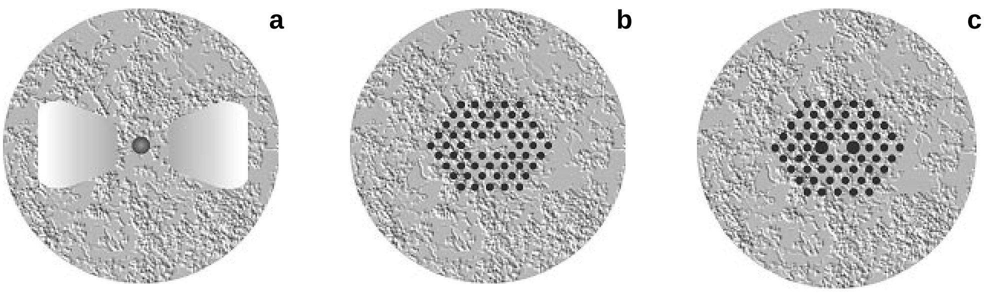

Fig. 1. Types of the HB fibers under investigation: *Fibercore* bow-tie – **a**, HB PCF (UMCS) – **b**, *BlazePhotonics* HB 1550 01 – **c**.

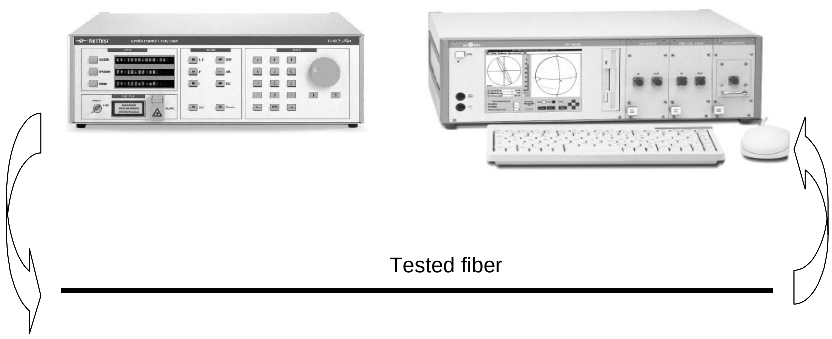

Fig. 2. Measurement setup.

in the center region of the fiber and made by putting three full silica glasses between silica tubes. The other HB PCF manufactured by *BlazePhotonics* (cat. no. HB 1550 01, see Fig. 1**c**), possesses 1-μm air holes near the core and additionally two 4-μm air holes situated close to the fiber core. This special arrangement of the silica tubes or holes with larger diameter near the core creates large difference between average refractive indices in two orthogonal directions.

The measuring setup (Fig. 2) included the tunable laser source Tunics PLUS operating within the wavelength range of 1500–1640 nm and the polarimeter PAT 9000B as the output state of polarization and power meter used in the configuration shown in Fig. 2.

The Jones matrix eigenanalysis method [9] was selected for the DGD measurements.

4. PMD in microstructured fibers

The beat length parameter versus wavelength was measured by the elastooptic method for each type of the highly birefringent fibers. The method consists in rolling of the iron cylinder along the tested fiber and simultaneous output state of polarization observation on the Poincarè sphere. The distance between two nearest positions of the cylinder for which we observed displacement of the output state of polarization on the Poincarè sphere and its return to the initial position corresponds to the beat length parameter:

$$L_B = \frac{2\pi}{\Delta\beta}. \tag{5}$$

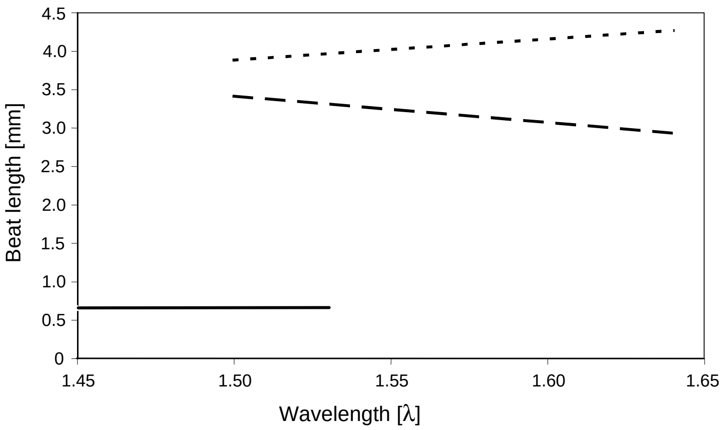

Fig. 3. Beat length as a function of wavelength for: HB PCF (UMCS) (solid line), *BlazePhotonics* PM 1550 01 (dashed line) and HB bow-tie (dotted line) fibers.

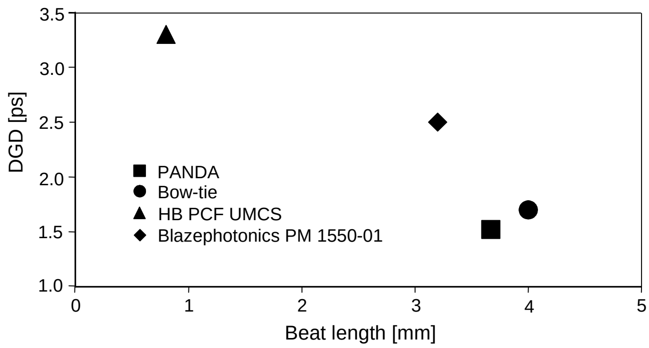

Fig. 4. Dependence of DGD on beat length for different types of HB fibers.

Results of the beat length measurements presented in Fig. 3 are generally in accordance with manufacturer data, but depending on the type of highly birefringent fibers totally different wavelength dependences were observed. While the beat length increases with wavelength in the bow-tie this behaviour is opposite for the *BlazePhotonics* HB PCF. This was independently confirmed elsewhere [10] for the HB PCF (UMCS) that revealed wavelength dependence of the beat length with opposite sign than the HB bow-tie fiber.

Dependence of the differential group delay value on the beat length parameter for different types of the fibers is shown in Fig. 4. For HB fibers beat length is of an order of single millimeters whereas the DGD parameter is relatively high. It is also evident that DGD depends on the modal birefringence and also on the phase birefringence. Both types of the HB PCF fibers have similar values of DGD but different beat lengths. The HB PCF (UMCS) has larger birefringence than *BlazePhotonics* PM 1550-01 but has smaller wavelength dependence of the beat length.

5. Influence of longitudinal strain

Influence of the longitudinal strain on the differential group delay for three different types of HB fiber samples was measured: 1.2 m long *BlazePhotonics* PM 1550 01, 75 cm long HB PCF (UMCS), and 78 cm long HB bow-tie fiber with average DGD values equal to 3.015 ps, 2.450, and 1.273 ps, respectively.

The longitudinal strain is the symmetrical type of the external perturbation. Based on Eqs. (4) and (5), it is possible to calculate DGD changes in the HB fiber under external longitudinal strain [11]:

$$\frac{\Delta\tau}{L} = \frac{\Delta\beta_0}{ck} + \varepsilon\frac{2\pi}{ckT_\varepsilon L_i}. \tag{6}$$

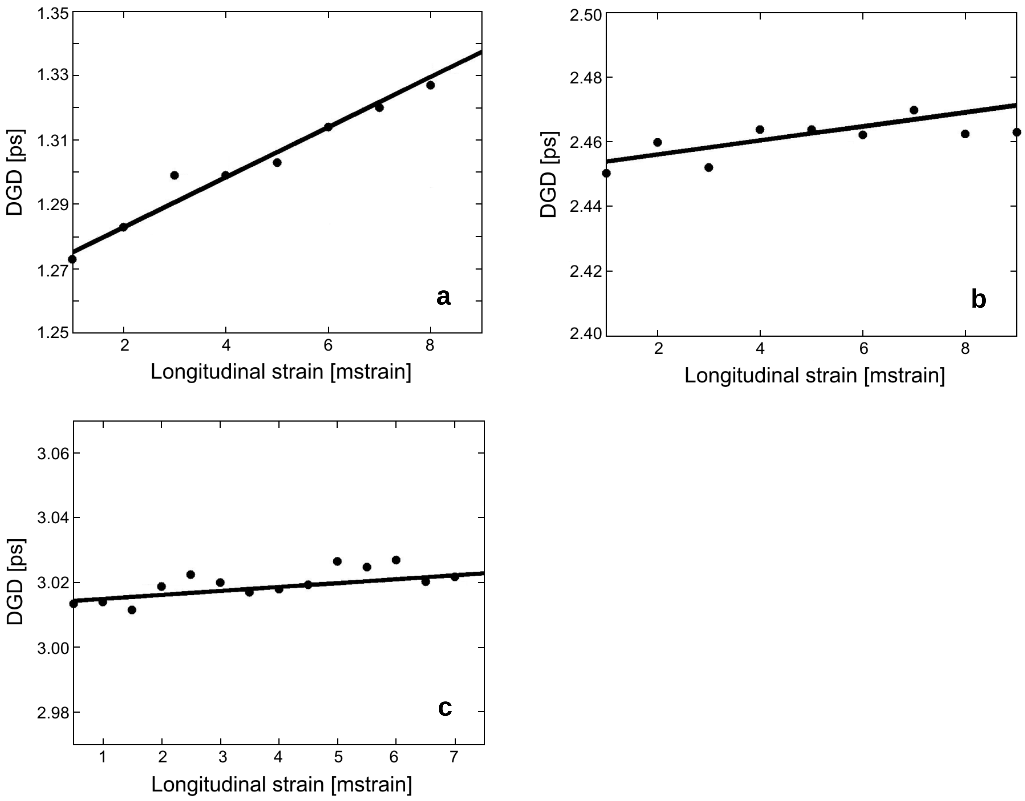

Fig. 5. DGD dependence on longitudinal strain for: bow-tie – **a**, HB PCF (UMCS) – **b**, *BlazePhotonics* PM 1550-01 – **c**.

The changes of DGD depend on the external perturbation. In our tests we measure the influence of longitudinal strain. Dots represent experimental data and lines represent theory (Fig. 5). We observe a good fit between theory and experiment. It appeared that DGD in the HB bow-tie fiber is the most strain sensitive and the largest strain-induced changes in DGD (12% for 10 mstrain) were obtained.

These results suggest that for the symmetrical external perturbation induced by longitudinal strain, PMD is being changed in the HB fibers exactly in the same way as birefringence. Consequently, the second “dispersive” term in Eq. (4) must be

T a b l e. Comparison of the measured HB fibers.

	Bow-tie	HB PCF (UMCS)	*BlazePhotonics*
Beat length [mm]	3.9	0.8	3.5
DGD [ps/m]	1.7	3.3	2.5
DGD changes under strain [10 mstrain]	12%	3.8%	~0%
Strain sensitivity [rad/mstrain×m]	78.5	11.2	~2.5

constant. On the other hand, it has been demonstrated [12] that temperature-induced changes in PMD are much bigger than those induced by birefringence.

Difference in DGD changes under longitudinal strain in the tested HB fibers and their strain sensitivities are summarized in the Table.

6. Influence of axial stress

We measured also the influence of axial stress on DGD in microstructured HB fibers (Fig. 6). Axial stress, an example of nonsymmetrical external perturbations, modifies the shape of the holes in microstructured fibers and in consequence changes their propagation properties. Since birefringence in the photonic crystal fiber results from the difference between average refractive indices in two orthogonal directions, small changes in the holes shape can increase or decrease internal birefringence of the fiber.

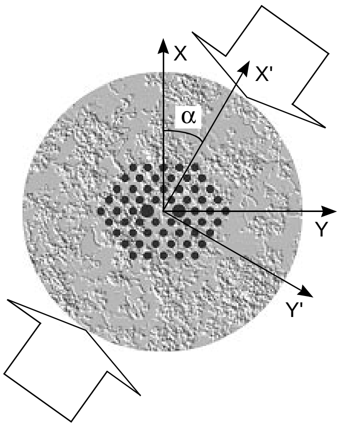

Fig. 6. Influence of axial stress that depends on the angle between birefringence axes and force direction.

Similarly to strain measurements axial stress-induced changes in DGD were measured for selected types of HB fibers: 12 cm long of *BlazePhotonics* PM 1550 01, 31 cm long HB PCF (UMCS) and 23 cm long of HB bow-tie fiber with average DGD value equal to 0.355, 0.984 and 0.386 ps, respectively.

These changes in the hole shape of the microstructured fibers modify both components of polarization mode dispersion described in Eq. (4), *i.e.*, chromatic dispersion and phase birefringence unlike in the case of longitudinal strain where only phase birefringence was modified. The changes of DGD value under external axial stress are the product of these two components. Elliptical holes in the microstructured fiber can increase the phase birefringence, assuming that the major axis of the ellipse is parallel to the *Y* axis (Fig. 6) and in consequence increase DGD (Fig. 7). Rotation at 90° decreases the value of DGD. This is a consequence of a decrease in the internal phase birefringence. In this case, the longer axis of ellipse is orthogonal to the *Y* axis. In *BlazePhotonics* PM 1550 01 fiber (see Fig. 7**a**) an increase of DGD value was

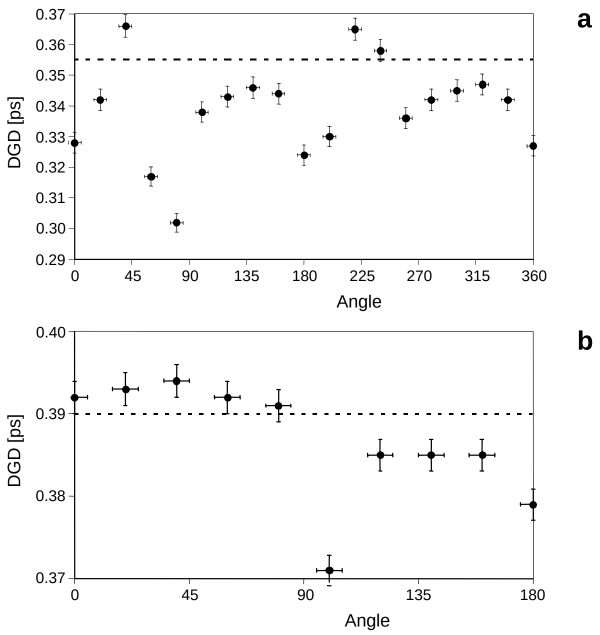

Fig. 7. DGD as a function of force direction for: **a** – *BlazePhotonics* PM 1550 01 and **b** – HB bow-tie fiber (dashed line represents the average value of non-stressed HB fiber).

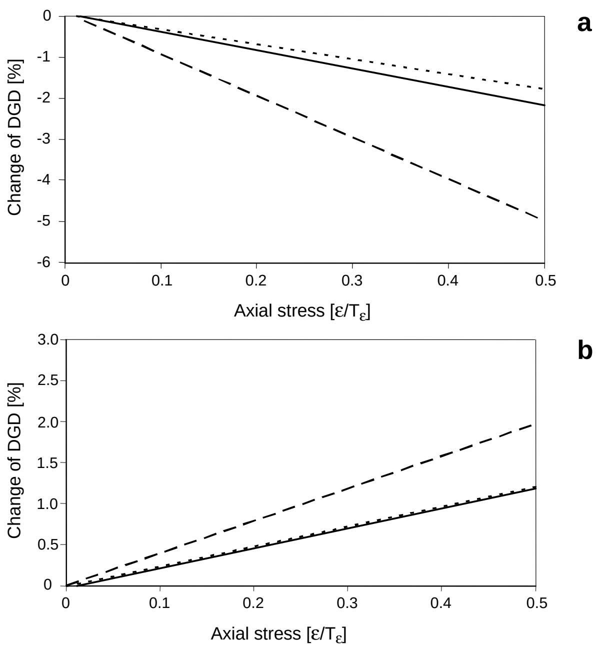

Fig. 8. Total change of DGD as a function of external stress for: **a** – 45 and **b** – 135 degrees between force direction and birefringence axes in the bow tie (dotted line), HB PCF (UMCS) (dashed line) and *BlazePhotonics* PM 1550 01 (solid line) HB fibers.

observed for small angle range (~40°). For HB bow-tie fiber (see Fig. 7**b**) the increase and decrease ranges of the DGD value were equal. A very low value of DGD for both types of fiber (near 90°, 180°, …) was caused by the coupling mode and in consequence the DGD value was compensated.

In the experiment, a change of the output state of polarization under external stress, visualized on the Poincarè sphere, was observed. Both fibers were measured under the same conditions – maximal stress value used was equal to induce a 2π phase shift of the polarized light observed at the output. The rate of $\varepsilon/T_\varepsilon$ was used to characterize the axial stress value. The influence of external stress on the phase birefringence in both types of HB fibers was compared. In PCF fibers a decrease (increase) of the DGD value higher than in HB bow-tie and HB PCF (UMCS) was observed (Fig. 7). This is a consequence of additional changes in chromatic dispersion for *BlazePhotonics* PM 1550 01 increases with a large change of the shape of the larger holes.

7. Conclusions

In this paper, PMD measurements in different types of microstructured fibers have been demonstrated and the influence of external perturbation such as those induced by longitudinal strain and axial stress on the PMD in HB fibers was determined. A good agreement between the theory and experimental data for longitudinal strain was obtained. Also, the coupling mode for axial stress with partial compensation of PMD was observed. The long-term aim of the studies is a perspective construction of a new all-fiber PMD compensator.

References

[1] Foschini G.J., Poole C.D., J. Lightwave Technol. **9** (1991), 1439.
[2] Lanne S., Corbel E., J. Lightwave Technol. **22** (2004), 1033.
[3] Urbańczyk W., Martynkien T., Bock W.J., Appl. Opt. **40** (2001), 1911.
[4] Tsai K.H., Kim K.S., Morse T.F., J. Lightwave Technol. **9** (1991), 7.
[5] Steel M.J., Osgood R.M., Jr., Opt. Lett. **26** (2001), 229.
[6] Ortigosa-Blanch A., Knight J.C., Wadsworth W., Arriaga J., Mangan B.J., Birks T.A., Russell P.St.J., Opt. Lett. **25** (2000), 1325.
[7] Hansen T.P., Broeng J., Libori S.E.B., Knudsen E., Bjarklev A., Jensen J.R., Simonsen H., Photon. Technol. Lett. **13** (2001), 588.
[8] Woliński T.R., *Polarimetric optical fibers and sensors*, [In] *Progress in Optics*, [Ed.] Emil Wolf, Vol. XL, North Holland, Amsterdam 2000, pp. 1–75.
[9] Heffner B.L., Photon. Technol. Lett. **4** (1992), 1066.
[10] Nasilowski T., Lesiak P., Kotynski R., Antkowiak M., Fernandez Fernandez A., Bergmans F., Thienpont H., *Birefringent photonic crystal fibers as a multi-parameter sensor*, [In] *Proc. IEEE/LEOS Benelux Chapt.*, Enschede 2003.
[11] Domański A.W., Lesiak P., Woliński T.R., Acta Phys. Pol. A **103** (2003), 221.
[12] Fontaine M., Wu B., Tzolov V.P., Bock W.J., Urbanczyk W., J. Lightwave Technol. **14** (1996), 585.

Received September 20, 2004
in revised form October 25, 2004